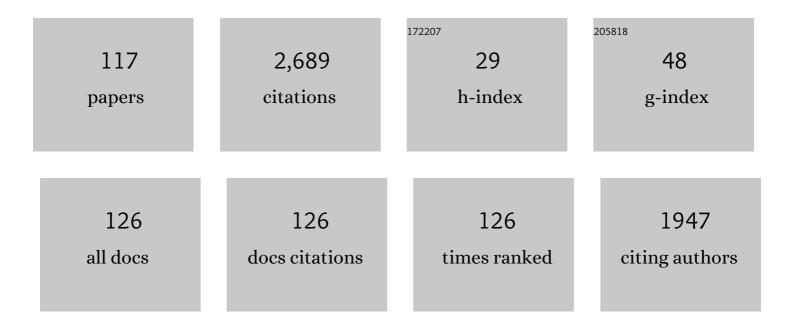
List of Publications by Year in descending order

Source: https://exaly.com/author-pdf/8726201/publications.pdf Version: 2024-02-01



WEIDEN LIN

#	Article	IF	CITATIONS
1	Low Coseismic Friction on the Tohoku-Oki Fault Determined from Temperature Measurements. Science, 2013, 342, 1214-1217.	6.0	254
2	Coseismic fluid–rock interactions at high temperatures in the Chelungpu fault. Nature Geoscience, 2008, 1, 679-683.	5.4	113
3	Stress State in the Largest Displacement Area of the 2011 Tohoku-Oki Earthquake. Science, 2013, 339, 687-690.	6.0	112
4	In situ stress state in the Nankai accretionary wedge estimated from borehole wall failures. Geochemistry, Geophysics, Geosystems, 2010, 11, .	1.0	105
5	Extreme hydrothermal conditions at an active plate-bounding fault. Nature, 2017, 546, 137-140.	13.7	84
6	Permanent strain of thermal expansion and thermally induced microcracking in Inada granite. Journal of Geophysical Research, 2002, 107, ECV 3-1-ECV 3-16.	3.3	76
7	Presentâ€day principal horizontal stress orientations in the Kumano forearc basin of the southwest Japan subduction zone determined from IODP NanTroSEIZE drilling Site C0009. Geophysical Research Letters, 2010, 37, .	1.5	76
8	High magnetic susceptibility of fault gouge within Taiwan Chelungpu fault: Nondestructive continuous measurements of physical and chemical properties in fault rocks recovered from Hole B, TCDP. Geophysical Research Letters, 2006, 33, .	1.5	75
9	Anelastic strain recovery reveals extension across SW Japan subduction zone. Geophysical Research Letters, 2009, 36, .	1.5	75
10	Localized rotation of principal stress around faults and fractures determined from borehole breakouts in hole B of the Taiwan Chelungpu-fault Drilling Project (TCDP). Tectonophysics, 2010, 482, 82-91.	0.9	69
11	Clay mineral reactions caused by frictional heating during an earthquake: An example from the Taiwan Chelungpu fault. Geophysical Research Letters, 2008, 35, .	1.5	66
12	Evidence of frictional melting from disk-shaped black material, discovered within the Taiwan Chelungpu fault system. Geophysical Research Letters, 2006, 33, .	1.5	61
13	Surface features of uniaxial tensile fractures and their relation to rock anisotropy in Inada granite. International Journal of Rock Mechanics and Minings Sciences, 2007, 44, 98-107.	2.6	57
14	Disturbance of deep-sea environments induced by the M9.0 Tohoku Earthquake. Scientific Reports, 2012, 2, 270.	1.6	55
15	A chemical kinetic approach to estimate dynamic shear stress during the 1999 Taiwan Chi hi earthquake. Geophysical Research Letters, 2007, 34, .	1.5	51
16	Subsurface structure, physical properties, fault-zone characteristics and stress state in scientific drill holes of Taiwan Chelungpu Fault Drilling Project. Tectonophysics, 2009, 466, 307-321.	0.9	51
17	Determination of three-dimensional in situ stresses from anelastic strain recovery measurement of cores at great depth. Tectonophysics, 2006, 426, 221-238.	0.9	50
18	Core Description and Characteristics of Fault Zones from Hole-A of the Taiwan Chelungpu-Fault Drilling Project. Terrestrial, Atmospheric and Oceanic Sciences, 2007, 18, 327.	0.3	50

#	Article	IF	CITATIONS
19	Characterization of slip zone associated with the 1999 Taiwan Chi-Chi earthquake: X-ray CT image analyses and microstructural observations of the Taiwan Chelungpu fault. Tectonophysics, 2008, 449, 63-84.	0.9	49
20	The State of Stress on the Fault Before, During, and After a Major Earthquake. Annual Review of Earth and Planetary Sciences, 2020, 48, 49-74.	4.6	49
21	Nondestructive continuous physical property measurements of core samples recovered from hole B, Taiwan Chelungpuâ€Fault Drilling Project. Journal of Geophysical Research, 2007, 112, .	3.3	45
22	Distribution of stress state in the Nankai subduction zone, southwest Japan and a comparison with Japan Trench. Tectonophysics, 2016, 692, 120-130.	0.9	45
23	Current stress state and principal stress rotations in the vicinity of the Chelungpu fault induced by the 1999 Chi hi, Taiwan, earthquake. Geophysical Research Letters, 2007, 34, .	1.5	41
24	Thermal properties and thermal structure in the deep-water coalbed basin off the Shimokita Peninsula, Japan. Marine and Petroleum Geology, 2016, 73, 445-461.	1.5	41
25	Integrating borehole-breakout dimensions, strength criteria, and leak-off test results, to constrain the state of stress across the Chelungpu Fault, Taiwan. Tectonophysics, 2010, 482, 65-72.	0.9	39
26	Dynamic process of turbidity generation triggered by the 2011 Tohokuâ€Oki earthquake. Geochemistry, Geophysics, Geosystems, 2012, 13, .	1.0	38
27	Fluid transport properties in sediments and their role in large slip near the surface of the plate boundary fault in the Japan Trench. Earth and Planetary Science Letters, 2013, 382, 150-160.	1.8	34
28	Thermal conductivities, thermal diffusivities, and volumetric heat capacities of core samples obtained from the Japan Trench Fast Drilling Project (JFAST). Earth, Planets and Space, 2014, 66, .	0.9	34
29	Petrophysical, Geochemical, and Hydrological Evidence for Extensive Fractureâ€Mediated Fluid and Heat Transport in the Alpine Fault's Hangingâ€Wall Damage Zone. Geochemistry, Geophysics, Geosystems, 2017, 18, 4709-4732.	1.0	31
30	High magnetic susceptibility produced in highâ€velocity frictional tests on core samples from the Chelungpu fault in Taiwan. Geophysical Research Letters, 2007, 34, .	1.5	29
31	Application of time domain reflectometry to determination of volumetric water content in rock. Water Resources Research, 1998, 34, 2623-2631.	1.7	27
32	Low total and inorganic carbon contents within the Taiwan Chelungpu fault system. Geochemical Journal, 2007, 41, 391-396.	0.5	26
33	Velocity dependence of shearâ€induced permeability associated with frictional behavior in fault zones of the Nankai subduction zone. Journal of Geophysical Research, 2012, 117, .	3.3	26
34	In-situ stress analysis using the anelastic strain recovery (ASR) method at the first offshore gas production test site in the eastern Nankai Trough, Japan. Marine and Petroleum Geology, 2015, 66, 418-424.	1.5	26
35	1,3-Dimethylurea Tetrabutylphosphonium Bromide Ionic Liquids for NO Efficient and Reversible Capture. Energy & Fuels, 2016, 30, 735-739.	2.5	26
36	Determination of stress state in deep subsea formation by combination of hydraulic fracturing in situ test and core analysis: A case study in the IODP Expedition 319. Journal of Geophysical Research: Solid Earth, 2013, 118, 1203-1215.	1.4	25

#	Article	lF	CITATIONS
37	In situ stress and pore pressure in the Kumano Forearc Basin, offshore SW Honshu from downhole measurements during riser drilling. Geochemistry, Geophysics, Geosystems, 2013, 14, 1454-1470.	1.0	23
38	Analyses of pseudotachylyte from Hole-B of Taiwan Chelungpu Fault Drilling Project (TCDP); their implications for seismic slip behaviors during the 1999 Chi-Chi earthquake. Tectonophysics, 2009, 469, 13-24.	0.9	22
39	Stress states at the subduction input site, Nankai Subduction Zone, using anelastic strain recovery (ASR) data in the basement basalt and overlying sediments. Tectonophysics, 2013, 600, 91-98.	0.9	22
40	Thermal conductivities under high pressure in core samples from IODP NanTroSEIZE drilling site C0001. Geochemistry, Geophysics, Geosystems, 2011, 12, n/a-n/a.	1.0	21
41	Determination of three-dimensional in situ stresses by anelastic strain recovery in Wenchuan Earthquake Fault Scientific Drilling Project Hole-1 (WFSD-1). Tectonophysics, 2014, 619-620, 123-132.	0.9	21
42	Transport properties and dynamic processes in a fault zone from samples recovered from TCDP Hole B of the Taiwan Chelungpu Fault Drilling Project. Geochemistry, Geophysics, Geosystems, 2009, 10, .	1.0	19
43	Scale dependence of <i>inâ€situ</i> permeability measurements in the Nankai accretionary prism: The role of fractures. Geophysical Research Letters, 2012, 39, .	1.5	19
44	Examination of gas hydrate-bearing deep ocean sediments by X-ray Computed Tomography and verification of physical property measurements of sediments. Marine and Petroleum Geology, 2019, 108, 239-248.	1.5	19
45	Quantification of free gas in the Kumano fore-arc basin detected from borehole physical properties: IODP NanTroSEIZE drilling Site C0009. Geochemistry, Geophysics, Geosystems, 2011, 12, n/a-n/a.	1.0	17
46	Principal horizontal stress orientations prior to the 2011 M <sub>w</sub> 9.0 Tohoku-Oki, Japan, earthquake in its source area. Geophysical Research Letters, 2011, 38, n/a-n/a.	1.5	14
47	Correction to "Principal horizontal stress orientations prior to the 2011 M <sub>w</sub> 9.0 Tohoku-Oki, Japan, earthquake in its source area― Geophysical Research Letters, 2011, 38, n/a-n/a.	1.5	14
48	Anisotropy of Thermal Property, Ultrasonic Wave Velocity, Strength Property and Deformability in Inada Granite. Journal of the Japan Society of Engineering Geology, 2003, 44, 175-187.	0.1	14
49	Porosity, permeability, and grain size of sediment cores from gas-hydrate-bearing sites and their implication for overpressure in shallow argillaceous formations: Results from the national gas hydrate program expedition 02, Krishna-Godavari Basin, India. Marine and Petroleum Geology, 2019, 108, 332-347.	1.5	13
50	Stability of novel cellulose-nanofiber-containing foam as environmentally friendly fracturing fluid. Journal of Petroleum Science and Engineering, 2022, 208, 109512.	2.1	13
51	CFD simulation on the generation of turbidites in deepwater areas: a case study of turbidity current processes in Qiongdongnan Basin, northern South China Sea. Acta Oceanologica Sinica, 2014, 33, 127-137.	0.4	12
52	Experimental Anelastic Strain Recovery Compliance of Three Typical Rocks. Rock Mechanics and Rock Engineering, 2014, 47, 1987-1995.	2.6	12
53	Stress state measured at ~7 km depth in the Tarim Basin, NW China. Scientific Reports, 2017, 7, 4503.	1.6	12
54	Indian Monsoonal Variations During the Past 80ÂKyr Recorded in NGHPâ€02 Hole 19B, Western Bay of Bengal: Implications From Chemical and Mineral Properties. Geochemistry, Geophysics, Geosystems, 2019, 20, 148-165.	1.0	12

#	Article	IF	CITATIONS
55	Pressure dependence of fluid transport properties of shallow fault systems in the Nankai subduction zone. Earth, Planets and Space, 2014, 66, .	0.9	11
56	Three-dimensional in situ stress determination by anelastic strain recovery and its application at the Wenchuan Earthquake Fault Scientific Drilling Hole-1 (WFSD-1). Science China Earth Sciences, 2014, 57, 1212-1220.	2.3	11
57	Depth dependence of the frictional behavior of montmorillonite fault gouge: Implications for seismicity along a décollement zone. Geophysical Research Letters, 2017, 44, 5383-5390.	1.5	11
58	Experimental and numerical investigation of the temperature response to stress changes of rocks. Journal of Geophysical Research: Solid Earth, 2017, 122, 5101-5117.	1.4	11
59	Extended hybrid pressure and velocity boundary conditions for D3Q27 lattice Boltzmann model. Applied Mathematical Modelling, 2012, 36, 2031-2055.	2.2	10
60	Porosity and permeability evolution and evaluation in anisotropic porosity multiscale-multiphase-multicomponent structure. Science Bulletin, 2012, 57, 320-327.	1.7	10
61	Strength characteristics of sediments from a gas hydrate deposit in the Krishna–Godavari Basin on the eastern margin of India. Marine and Petroleum Geology, 2019, 108, 348-355.	1.5	10
62	Profiles of volumetric water content in fault zones retrieved from hole B of the Taiwan Chelungpuâ€fault Drilling Project (TCDP). Geophysical Research Letters, 2008, 35, .	1.5	9
63	Anelastic Strain Recovery Method to Determine Inâ€situ Stresses and an Application Example. Chinese Journal of Geophysics, 2012, 55, 333-342.	0.2	9
64	Change of Microcrack Widths induced by Temperature Increase in Inada Granite Journal of the Japan Society of Engineering Geology, 1995, 36, 300-304.	0.1	9
65	Changes in paleostress and its magnitude related to seismic cycles in the Chelungâ€pu Fault, Taiwan. Tectonics, 2015, 34, 2418-2428.	1.3	8
66	Stress buildup and drop in inland shallow crust caused by the 2011 Tohoku-oki earthquake events. Scientific Reports, 2017, 7, 10242.	1.6	8
67	Recovery of Stress During the Interseismic Period Around the Seismogenic Fault of the 1995 <i>M</i> <sub><i>w</i></sub> 6.9 Kobe Earthquake, Japan. Geophysical Research Letters, 2018, 45, 12,814.	1.5	8
68	Geometrical dependence on the stress and slip tendency acting on the subduction megathrust of the Nankai seismogenic zone off Kumano. Progress in Earth and Planetary Science, 2019, 6, .	1.1	8
69	Constraints on the fluid supply rate into and through gas hydrate reservoir systems as inferred from pore-water chloride and in situ temperature profiles, Krishna-Godavari Basin, India. Marine and Petroleum Geology, 2019, 108, 368-376.	1.5	8
70	Thermal Conductivity Profile in the Nankai Accretionary Prism at IODP NanTroSEIZE Site C0002: Estimations From Highâ€Pressure Experiments Using Input Site Sediments. Geochemistry, Geophysics, Geosystems, 2020, 21, e2020GC009108.	1.0	8
71	Equivalent Channel Models for Permeability Estimation and Their Application to Sedimentary Rocks Journal of the Japan Society of Engineering Geology, 1999, 39, 533-539.	0.1	8
72	Permeability of Inada Granite with High Temperature History and Its Estimation by the Equivalent Channel Models Journal of the Japan Society of Engineering Geology, 1999, 40, 25-35.	0.1	8

#	Article	IF	CITATIONS
73	Stress State in the Kumano Basin and in Slope Sediment Determined From Anelastic Strain Recovery: Results From IODP Expedition 338 to the Nankai Trough. Geochemistry, Geophysics, Geosystems, 2017, 18, 3608-3616.	1.0	7
74	The Feature of Uniaxial Tensile Fractures in Granite and Their Relation to Rock Anisotropy. Journal of the Japan Society of Engineering Geology, 2005, 46, 227-231.	0.1	7
75	Tensile strength and deformability of Inada granite and their anisotropy: Comparison between uniaxial tension test and Brazilian test. Japanese Geotechnical Journal, 2008, 3, 165-173.	0.0	6
76	Pore Size Distribution of Rocks Determined by Mercury Intrusion Porosimetry. Journal of the Japan Society of Engineering Geology, 2016, 57, 201-212.	0.1	6
77	Stress-state differences between sedimentary cover and basement of the Songliao Basin, NE China: In-situ stress measurements at 6–7 km depth of an ICDP Scientific Drilling borehole (SK-II). Tectonophysics, 2020, 777, 228337.	0.9	6
78	Comparison of the Permeabilities of Shirahama Sandstone Specimens Jacketed with Different Methods Journal of the Japan Society of Engineering Geology, 1999, 40, 299-305.	0.1	6
79	On Visualization of Inner Microstructure in Rocks by Micro Focus X ray CT Journal of the Japan Society of Engineering Geology, 2002, 43, 235-238.	0.1	5
80	Chemical and isotopic characteristics of interstitial fluids within the Taiwan Chelungpu fault. Geochemical Journal, 2007, 41, 97-102.	0.5	5
81	Deformability of Several Granitic Rocks and Gabbros in Uniaxial Tension. Zairyo/Journal of the Society of Materials Science, Japan, 2007, 56, 654-659.	0.1	5
82	Equivalent formation strength as a proxy tool for exploring for the location and distribution of gas hydrates. Marine and Petroleum Geology, 2019, 108, 356-367.	1.5	5
83	Formation of excess fluid pressure, sediment fluidization and mass-transport deposits in the Plio-Pleistocene Boso forearc basin, central Japan. Geological Society Special Publication, 2019, 477, 255-264.	0.8	5
84	Cultivation-Based Characterization of Microbial Communities Associated with Deep Sedimentary Rocks from Taiwan Chelungpu Drilling Project Cores. Terrestrial, Atmospheric and Oceanic Sciences, 2007, 18, 395.	0.3	5
85	Permeability Measurement Techniques for Intermediate Principal Stress Direction. Journal of the Japan Society of Engineering Geology, 2002, 43, 43-48.	0.1	5
86	Vitrinite reflectance and consolidation characteristics of the postâ€middle Miocene Forearc Basin in central and eastern Boso Peninsula, central Japan: Implications for basin subsidence. Island Arc, 2020, 29, e12344.	0.5	4
87	A Method for Core Reorientation Based on Rock Remanent Magnetization: Application to Hemipelagic Sedimentary Soft Rock. Materials Transactions, 2020, 61, 1638-1644.	0.4	4
88	Determining In-Situ Stress State by Anelastic Strain Recovery Method Beneath Xiamen: Implications for the Coastal Region of Southeastern China. Rock Mechanics and Rock Engineering, 2022, 55, 5687-5703.	2.6	4
89	Evaluating Stress State, Physical Properties, and Rupturing Behavior of Seismogenic Faults through Scientific Drillings. Journal of Geography (Chigaku Zasshi), 2017, 126, 223-246.	0.1	3
90	Difference of the Surface Roughness due to the Orientation of the Rock Fabrics in Inada Granite, Measured by Digital Photogrammetry. Journal of the Japan Society of Engineering Geology, 2006, 47, 252-258.	0.1	3

#	Article	IF	CITATIONS
91	Delay Effect on Advection and Diffusion Phenomena by Physicochemical Change of Pore Water in Nanopores. Journal of the Japan Society of Engineering Geology, 2004, 45, 118-124.	0.1	3
92	Strain Softening of Siltstones in Consolidation Process. Materials Transactions, 2020, 61, 1096-1101.	0.4	3
93	Correction to "A chemical kinetic approach to estimate dynamic shear stress during the 1999 Taiwan Chi-Chi earthquake― Geophysical Research Letters, 2008, 35, .	1.5	2
94	Electrical resistivity measurements of rocks under confining pressure condition. JAMSTEC Report of Research and Development, 2017, 24, 1-9.	0.2	2
95	Application of core-based stress measurement methods:. Journal of the Japanese Association for Petroleum Technology, 2017, 82, 428-437.	0.0	2
96	IDENTIFYING ANISOTROPIC IN SITU STRESS CONDITION AND ITS IMPACT ON DISPLACEMENT PROFILES FOR TUNNELING WITH HIGH OVERBURDEN. Journal of Japan Society of Civil Engineers Ser F1 (Tunnel) Tj ETQq0 0 0	rgB <b>Ð/Ø</b> ver	loc <b>k</b> 10 Tf 50
97	Determination of horizontal stress orientations from borehole breakout analyses in an ocean drilling project. , 2013, , .		1
98	Summary of the Japan Trench Fast Drilling Project (JFAST) and its Main Achievements. Journal of the Japan Society of Engineering Geology, 2014, 55, 241-250.	0.1	1
99	Strain Softening of Siltstones in Consolidation Process. Zairyo/Journal of the Society of Materials Science, Japan, 2020, 69, 250-255.	0.1	1
100	Thermal conductivity changes in subducting basalt, Nankai subduction zone, SW Japan: An estimation from laboratory measurements under separate high-pressure and high-temperature conditions. , 0, , .		1
101	Porosity profile within the Taiwan Chelungpu Fault, reconstructed from X-ray computed tomography images. JAMSTEC Report of Research and Development, 2009, 9, 2_15-2_22.	0.2	1
102	Theoretical Investigation on New Analyzing Procedure of Anelastic Strain Recovery Method for Stress Measurements Based on Bayesian Statistical Modeling. Materials Transactions, 2021, , .	0.4	1
103	Construction of rock physics model based on electrical conductivity characteristics of rock samples obtained in seafloor hydrothermal areas. BUTSURI-TANSA(Geophysical Exploration), 2018, 71, 43-55.	0.0	1
104	An Ancient >200Âm Cumulative Normal Faulting Displacement Along the Futagawa Fault Dextrally Ruptured During the 2016 Kumamoto, Japan, Earthquake Identified by a Multiborehole Drilling Program. Geochemistry, Geophysics, Geosystems, 2022, 23, .	1.0	1
105	Spatial and Temporal Stress Variations before and after the 2008 Wenchuan <i>M</i> <sub>w</sub> 7.9 Earthquake and its Implications: A Study based on Borehole Stress Data. Acta Geologica Sinica, 2023, 97, 226-242.	0.8	1
106	Micro-pore Visualization and their Quantitative Analysis using Atomic Force Microscope Journal of the Japan Society of Engineering Geology, 2001, 42, 24-29.	0.1	0
107	Thermal properties of the hanging wall of the central Alpine Fault, New Zealand. New Zealand Journal of Geology, and Geophysics, 2020, , 1-12.	1.0	0
108	Theoretical Investigation on New Analyzing Procedure of Anelastic Strain Recovery Method for Stress Measurements based on Bayesian Statistical Modeling. Zairyo/Journal of the Society of Materials Science, Japan, 2021, 70, 573-580.	0.1	0

#	Article	IF	CITATIONS
109	The Effects of Salinity of Pore Water on Apparent Dielectric Constant and Resistivity in Sands Journal of the Japan Society of Engineering Geology, 2001, 42, 140-148.	0.1	0
110	Applications of anelastic strain measurements in scientific ocean deep drillings. , 2010, , 199-204.		0
111	Experimental Study of Hydraulic Conductivity and Hydraulic Gradient in Rock Specimen. Journal of Japanese Association of Hydrological Sciences, 1999, 29, 205-214.	0.2	0
112	Effects of Probe Installation Method, Crack Existence and High Temperature on Apparent Dielectric Constant Determined by Time Domain Reflectometry in Rocks. Journal of Japanese Association of Hydrological Sciences, 1999, 29, 189-204.	0.2	0
113	A Case Study of Three-dimensional Determination of Stress Orientation to Crystalline Rock Samples in Wenchuan Earthquake Fault Scientific Drilling Project Hole-2. , 2015, , 87-90.		0
114	A Method for Core Reorientation Based on Rock Remanent Magnetization:Application to Hemipelagic Sedimentary Soft Rock. Zairyo/Journal of the Society of Materials Science, Japan, 2020, 69, 256-262.	0.1	0
115	Measurements of Post-seismic Stress State to 700 Meters Depth Using Anelastic Strain Recovery Method in Source Area of the 2016 Kumamoto Earthquakes. Journal of the Japan Society of Engineering Geology, 2021, 62, 13-22.	0.1	0
116	Compressive Strength of a Pliocene Sedimentary Soft Rock Retrieved from Nankai Trough Ocean Drillings. Zairyo/Journal of the Society of Materials Science, Japan, 2022, 71, 251-258.	0.1	0
117	Calculation of P-Wave Velocity in Sandstones with Different Pore Size Distributions Using Digital Rock Model without Segmentation. Zairyo/Journal of the Society of Materials Science, Japan, 2022, 71, 235-242.	0.1	0